

Radio frequency cavities:

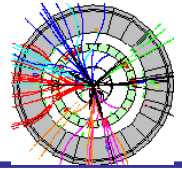
- electromagnetic waves & modes
- phase/group velocity & dispersion diagram
- cavity resonators & quality factors
- transit-time factor
- iris-loaded structures
- RF power generation & coupling

Imperfections:

- closed-orbit distortions & bumps
- sources of distortions
- gradient errors
- resonant condition
- multipoles / chromaticity



Electromagnetic waves in free space

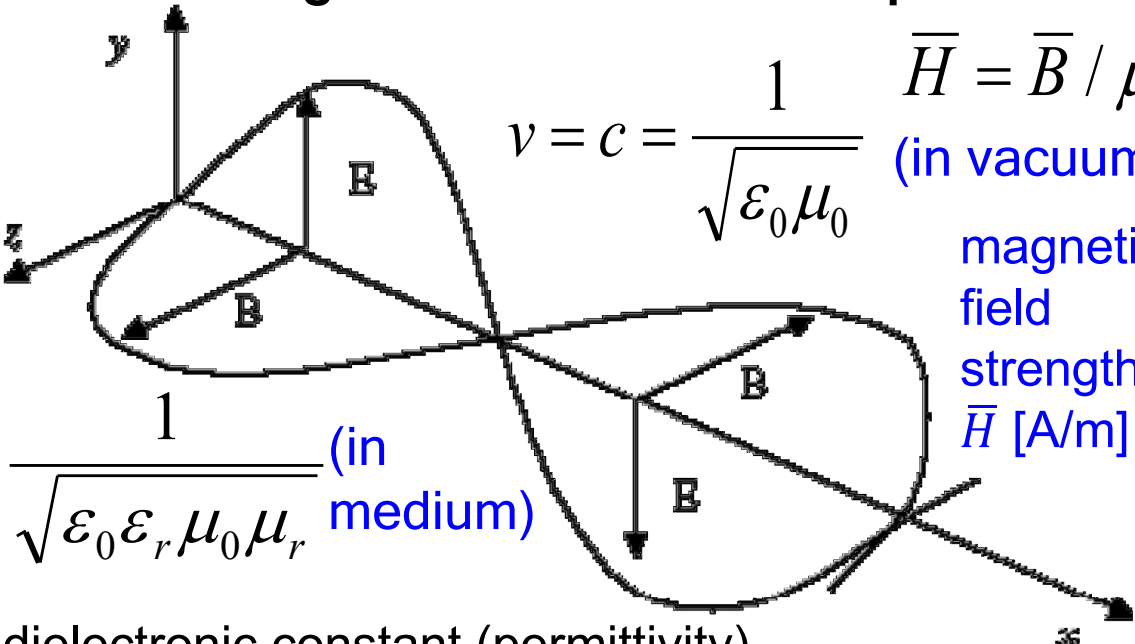


Maxwell's equation: $\nabla \times \bar{E} = -\frac{\partial \bar{B}}{\partial t}$ magnetic flux: \bar{B} [T]

in integral form: $\oint \bar{E} \cdot d\bar{s} = -\frac{d}{dt} \int_S \bar{B} \cdot \bar{n} da$

→ no continuous acceleration if no time-dependent magnetic field. 2 ways: time-dependent magnetic field or electromagnetic field oscillating in resonant cavities.

Electromagnetic waves in free space:



$\bar{H} = \bar{B} / \mu$ (in vacuum)

magnetic field strength: \bar{H} [A/m]

$v = c = \frac{1}{\sqrt{\epsilon_0 \mu_0}}$

$v = \frac{1}{\sqrt{\epsilon_0 \epsilon_r \mu_0 \mu_r}}$ (in medium)

ϵ_r = dielectric constant (permittivity)

μ_r = magnetic permeability

Poynting vector or

ratio of electric & magnetic field: local power flux:

$E/H = 376.6 \sqrt{\mu_r / \epsilon_r}$ [ohm] $\bar{P} = (\bar{E} \times \bar{H}) [\text{Wm}^{-2}]$

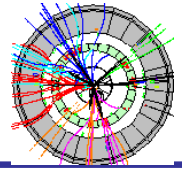
why not electromagnetic fields in free space? 2 reasons:

a) electric field normal to direction of propagation

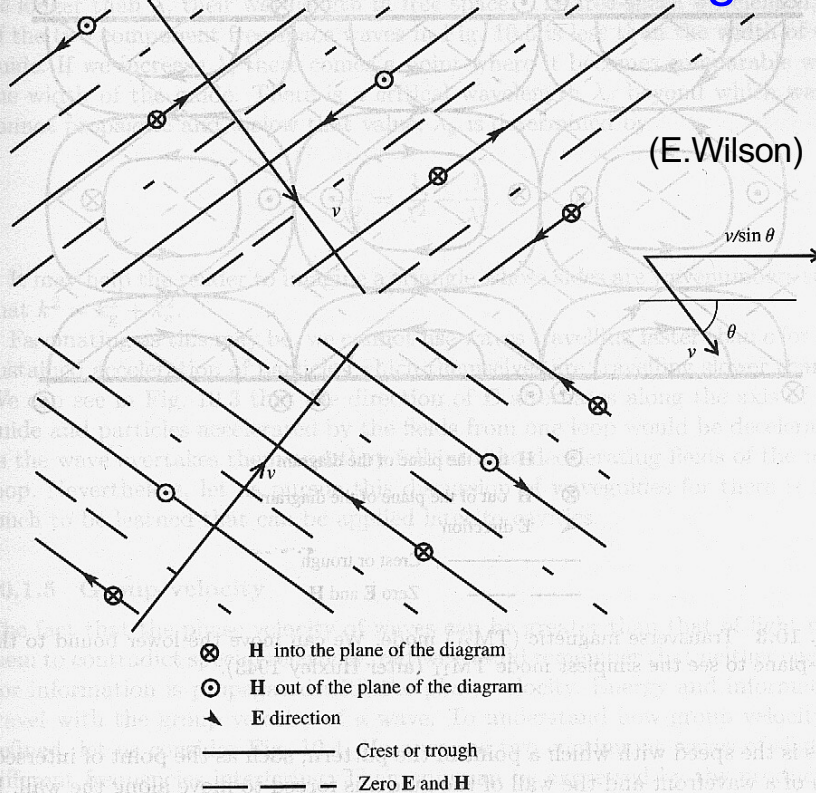
b) high energy particles slip behind accelerating phase since free wave propagates at velocity of light c .



Electromagnetic waves in guides

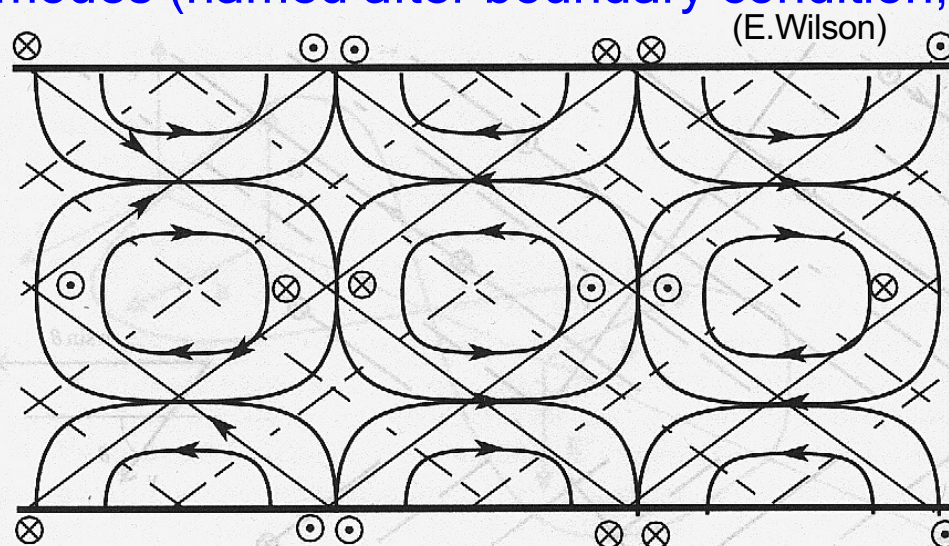


let's examine two traveling waves in a guide



phase velocity
 (“speed of a point
 in the pattern”)
 $v/\sin\theta > v$ to
 satisfy boundary
 conditions. $v = c$
 for an electro-
 magnetic wave
 (analogous to a
 surf board traver-
 sing a beach with
 a speed higher
 than the waves)

superposition of 2 waves gives transverse magnetic
 modes (named after boundary condition, here TM_{21})



wavelength
 in guide $\lambda_g >$
 wavelength
 in free space
 λ . related by
 the “critical”
 wavelength
 λ_c (beyond
 which waves

boundary conditions:

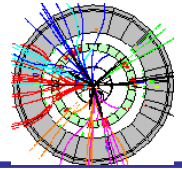
$$\vec{n} \times \vec{E} = 0$$

$$\vec{n} \cdot \vec{H} = 0$$

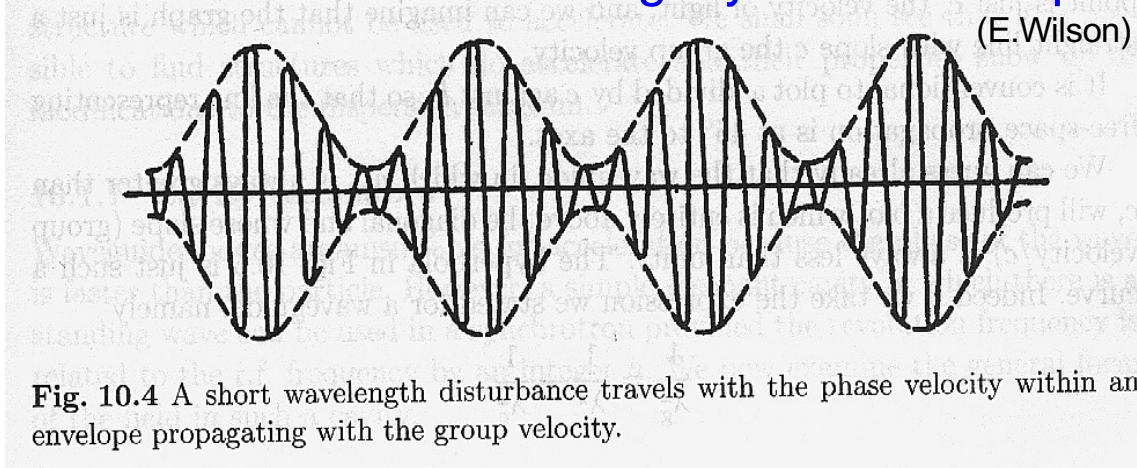
⊙ H into the plane of the diagram
 ⊗ H out of the plane of the diagram
 → E direction
 — Crest or trough
 - - - Zero E and H

$$\frac{1}{\lambda_g^2} = \frac{1}{\lambda^2} - \frac{1}{\lambda_c^2}$$

do not
 propa-
 gate)



Interference of 2 waves with slightly different frequency



$$\begin{aligned}
 E &= E_0 \sin[(k + dk)x - (\omega + d\omega)t] \\
 &+ E_0 \sin[(k - dk)x - (\omega - d\omega)t] \\
 &= 2E_0 \sin[kx - \omega t] \cos[dkx - d\omega t] \\
 &= 2E_0 f_1(x, t) f_2(x, t) \quad k = 2\pi / \lambda
 \end{aligned}$$

$$f_1(x, t) = \sin[kx - \omega t] \quad kx - \omega t = \text{const.}$$

$$v_p = - \frac{df_1(x, t) / dt}{df_1(x, t) / dx} = \frac{\omega}{k}$$

phase velocity. carries
no info on modulation
or energy (no violation
of special relativity)

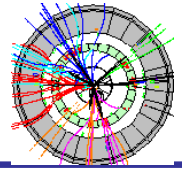
$$f_2(x, t) = \cos[xdk - td\omega] \quad xdk - td\omega = \text{const.}$$

$$v_g = - \frac{df_2(x, t) / dt}{df_2(x, t) / dx} = \frac{d\omega}{dk}$$

group velocity.
describes here
envelope of pattern



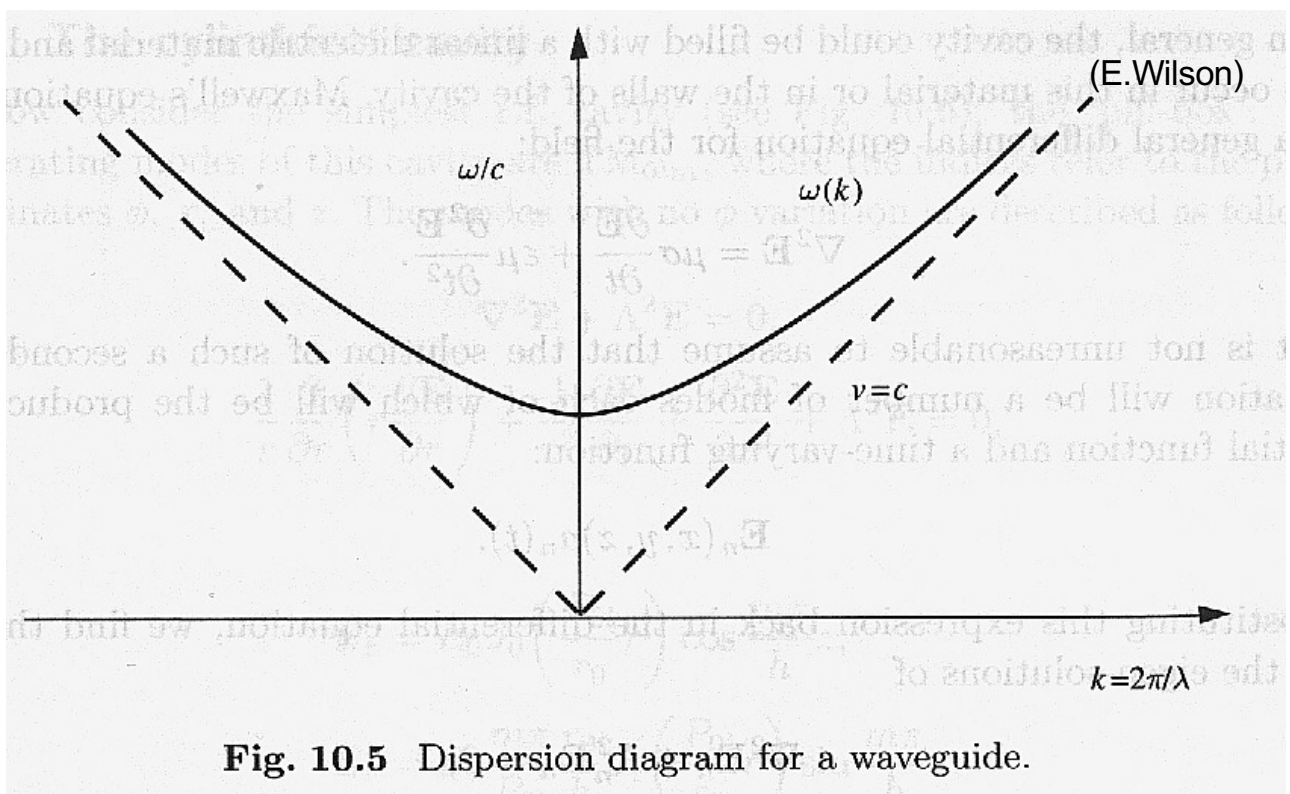
Dispersion diagram



Describe propagation by frequency vs. wavenumber:

$$\frac{1}{\lambda_g^2} = \frac{1}{\lambda^2} - \frac{1}{\lambda_c^2} \quad k = 2\pi / \lambda_g$$

$$\begin{aligned} 2\pi c / \omega &= \lambda \\ 2\pi c / \omega_c &= \lambda_c \end{aligned} \Rightarrow \left(\frac{\omega}{c} \right)^2 = k^2 + \left(\frac{\omega_c}{c} \right)^2$$

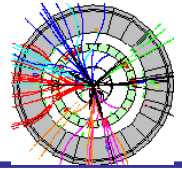


$v_p = \omega / k$ (slope) & $v_g = d\omega / dk$ (change of slope)

Small k indicate long wavelength when $v_p > c$. Notice that v_g decreases with k & at critical wavelength λ_c no energy flows along guide. The dispersion diagram must be modified by a suitable accelerating structure choice to have continuous acceleration of particles.



Cavity resonators



Waveguide unsuitable since phase velocity faster than particle, however resonant cavity with standing waves can be used to accelerate if revolution frequency f an integer multiple h of RF frequency f_{RF} . Study general case with linear dielectric material with losses in walls.

$$\nabla^2 E = \mu\sigma \frac{\partial E}{\partial t} + \varepsilon\mu \frac{\partial^2 E}{\partial t^2} \quad \begin{array}{l} \sigma \text{ finite conductivity} \\ \mu = \mu_r \mu_0 \text{ \& } \varepsilon = \varepsilon_r \varepsilon_0 \end{array}$$

Solution has spatial $E_n(x, y, z)$ & time component $a_n(t)$.
 E_n eigen-solutions of: $\nabla^2 E_n + \Lambda_n^2 E_n = 0$

where Λ_n related to resonant frequencies of modes.

Solution depends also on boundary conditions.

If conductivity losses in walls small enough:

$$\vec{n} \times \vec{E} = 0 \quad \vec{n} \cdot \vec{H} = 0$$

For time component $a_n(t)$ get differential equation:

$$\ddot{a}_n(t) + \frac{\sigma}{\varepsilon} \dot{a}_n(t) + \frac{\Lambda_n^2}{\varepsilon\mu} a_n(t) = 0 \quad \Rightarrow \quad \begin{array}{l} A_1 \text{ \& } A_2 \\ \text{depend} \\ \text{on initial} \\ \text{condition} \end{array}$$

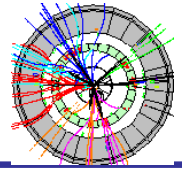
$$a_n(t) = e^{-\alpha_n t} \{A_1 \cos \Omega_n t + A_2 \sin \Omega_n t\}$$

where Ω_n resonant frequency of lossy cavity related to lossless frequency $\omega_n = \Lambda_n / \sqrt{\varepsilon\mu}$ & quality factor Q

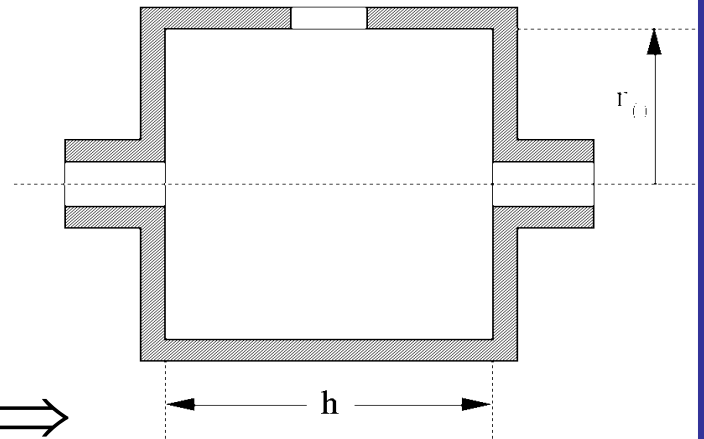
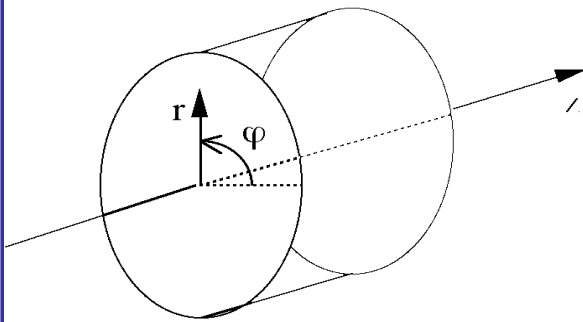
$$\Omega_n = \omega_n \sqrt{1 - \frac{1}{4Q^2}} \quad \begin{array}{l} \text{attenuation} \\ \text{constant:} \end{array} \quad \alpha_n = \frac{\sigma}{2\varepsilon} = \frac{\omega_n}{2Q}$$



The cylindrical cavity



Most simple RF cavity – pill box. Accelerating modes are the transverse magnetic modes (TM_{0lm}) of the cavity, where indices refer to polar coordinates ϕ, r & z .



$$\nabla^2 \bar{E} + \Lambda^2 \bar{E} = 0 \Rightarrow$$

$$\frac{1}{r} \frac{\partial}{\partial r} \left(r \frac{\partial \bar{E}}{\partial r} \right) + \frac{1}{r^2} \frac{\partial^2 \bar{E}}{\partial \phi^2} + \frac{\partial^2 \bar{E}}{\partial z^2} + \Lambda^2 \bar{E} = 0$$

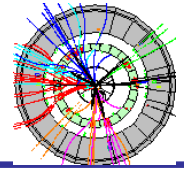
$$E_z = F(r) \cdot j(z); \quad E_r = Y(r) \cdot f(z)$$

$$\left\{ \begin{array}{l} E_z = E_0 J_0 \left(\frac{P_{0l}}{r_0} r \right) \cos \left(\frac{m\pi}{h} z \right) \\ E_r = E_0 \frac{m\pi}{P_{0l}} \frac{r_0}{h} J_1 \left(\frac{P_{0l}}{r_0} r \right) \sin \left(\frac{m\pi}{h} z \right) \\ \Lambda_{0lm}^2 = \left(\frac{P_{0l}}{r_0} \right)^2 + \left(\frac{m\pi}{h} \right)^2 \end{array} \right.$$

J_0 & J_1 Bessel functions of order 0 & 1, P_{0l} argument of Bessel function. J_0 ensures that electric field parallel to wall = 0. h cavity length & r_0 its radius.



The cylindrical cavity



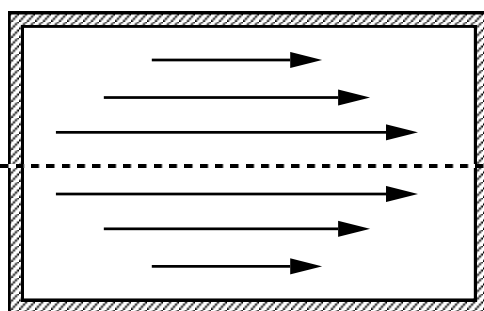
Second index l gives radial variation while third index m controls number of half-wavelengths in z direction. Numerical solution for energy, eigenvalue, lossless frequency & wavelength for $l = 1$ & $m = 0$ so-called “fundamental” transverse magnetic mode ($P_{0l} = 2.405$):

$$E = E_0 J_0\left(\frac{2.405r}{r_0}\right); \Lambda_{010} = \frac{2.405}{r_0}; \omega_{010} = \Lambda_{010} c$$

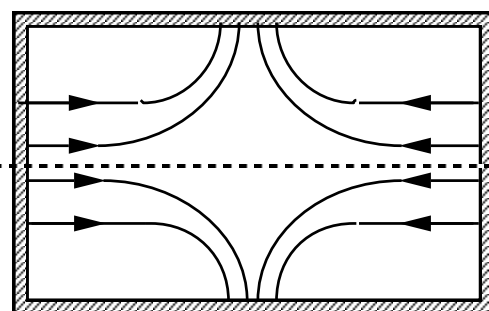
$$f_{010} = \frac{\omega_{010}}{2\pi} = \frac{2.405 c}{2\pi r_0}; \lambda_{010} = \frac{c}{f_{010}} = \frac{2\pi r_0}{2.405}$$

and $H_\theta = H_0 J_1(2.405r/r_0)$

Electrical field lines of (a) $l = 1 / m = 0$ (b) $l = 1 / m = 1$



(a)



(b)

Conductive surfaces:

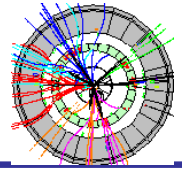
Surface resistance: $R_{surf} = 1/\sigma\delta_{surf}$ f_{RF} is RF frequency & σ materials' surface conductivity

Skin depth: $\delta_{surf} = 1/\sqrt{\pi f_{RF} \mu \sigma}$

surface conductivity



Quality factors



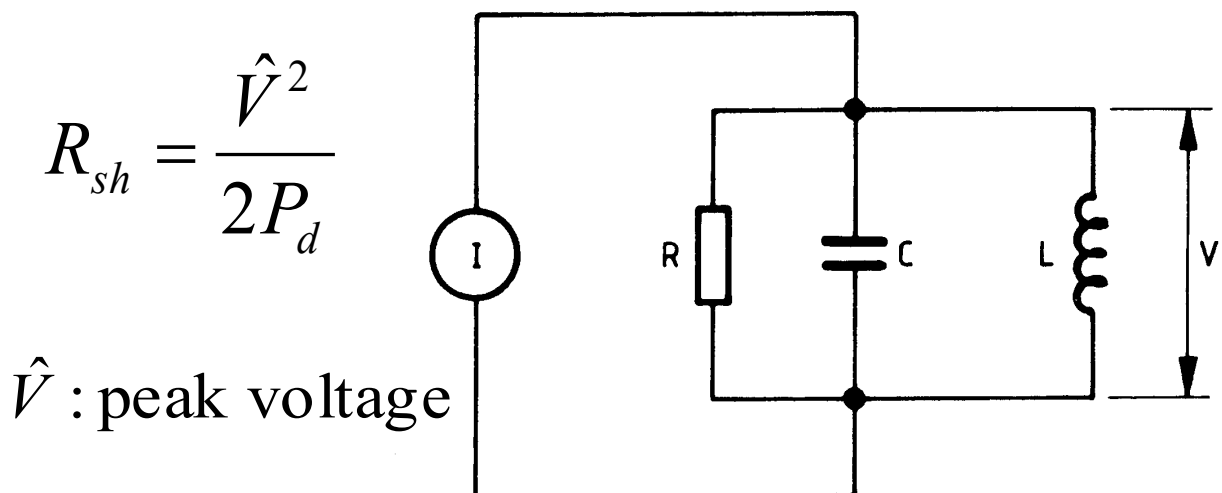
Quality factor Q of resonator defined as ratio of stored W_s & dissipated W_d energy per cycle (multiplied by 2π).

$$Q = \frac{W_s}{W_d} = \omega \frac{W_s}{P_d}, \quad W_s = \frac{\epsilon_0}{2} \int |E|^2 dV \quad \text{or} \quad \frac{\mu_0}{2} \int |H|^2 dV$$

First evaluate linear current density \vec{j} along cavity walls assuming lossless & losses introduced via conductivity σ of walls. Perfect conductor: $\vec{j} = \vec{n} \times \vec{H}$

$$P_d = \frac{R_{surf}}{2} \int_{surf} |H|^2 dsurf \quad \left(\text{for Cu } R_{surf} = 2.61 \cdot 10^{-7} \sqrt{\omega} [\Omega] \right)$$

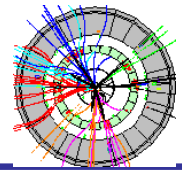
Cavity design programs does the estimates. Cavity can be approximated by shunt circuit as shown below \Rightarrow figure of merit of cavity shunt resistance R_{sh}



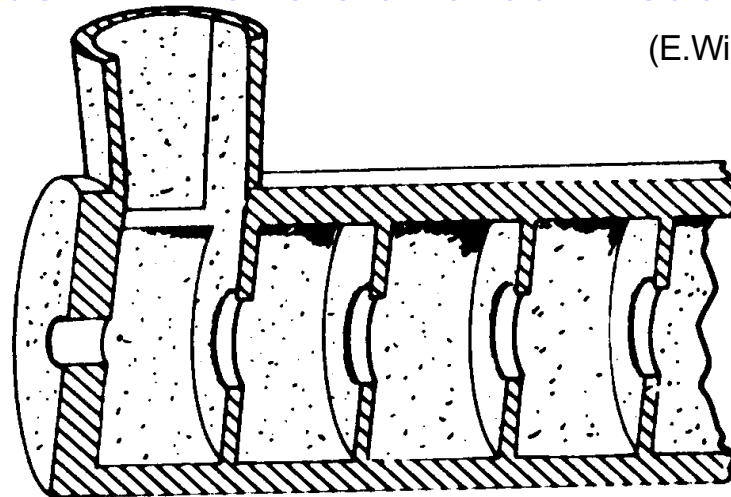
Voltage defined like $V = \int_{path} |E_z(x, y, z)| dl$



Iris-loaded structures



Most RF systems based of cavity series \approx a number of pill-boxes weakly coupled via beam aperture (“iris”). Electric fields will interfere & reflect in such a system.



(E.Wilson)

In iris-loaded structures dispersion diagram different, now $v_p < c$ in large k intervals. For particle acceleration first upward slope ($k \in [0, \pi/d]$) of function most useful:

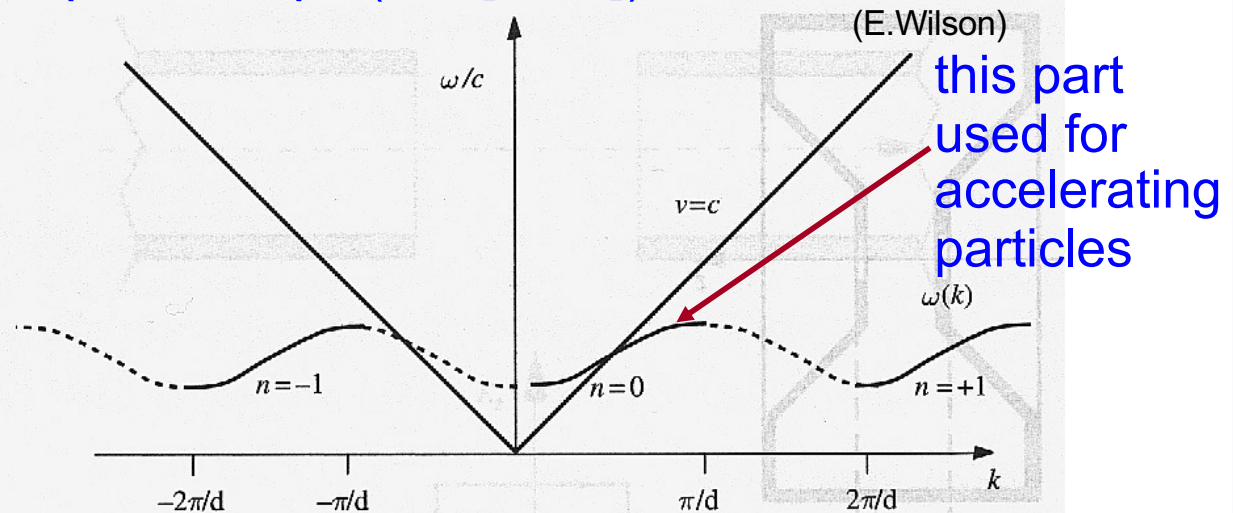
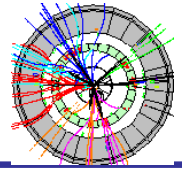


Fig. 10.10 Dispersion diagram for a loaded waveguide.

By symmetry, fields in each cavity have same form & can only differ in phase. Representing electric field of an infinitely long chain of cavities as space harmonic series $\Rightarrow k_n = k_0 + 2n\pi/d$ for n^{th} harmonic \Rightarrow dispersion curve periodic in $2n\pi/d \Rightarrow v_p < c$ inevitably somewhere.



Accelerators have many cavities \Rightarrow must synchronize spacing L for bunch to arrive at same phase at each cavity. Alvarez linac: increasing L with increased β .

$$L = \beta\lambda$$

λ = free-space wave length of RF excitations

Don't use standing-wave configurations but patterns repeating over > 1 cell. Below patterns repeating over 6 & 3 cavities corresponding to $\pi/3$ & $2\pi/3$ phase change, 2nd safely on sloping part of dispersion curve.

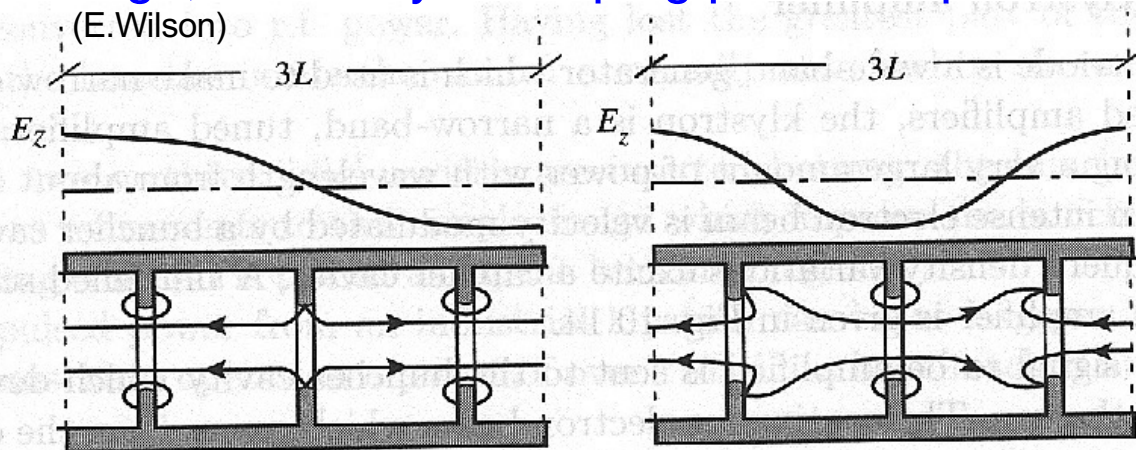


Fig. 10.13 Modes of a multicell cavity.

(E.Wilson)

Coupling of RF power to cavity:

Loops placed in regions of cavity where magnetic field stronger since loop have common component with magnetic field mode aimed to be created.

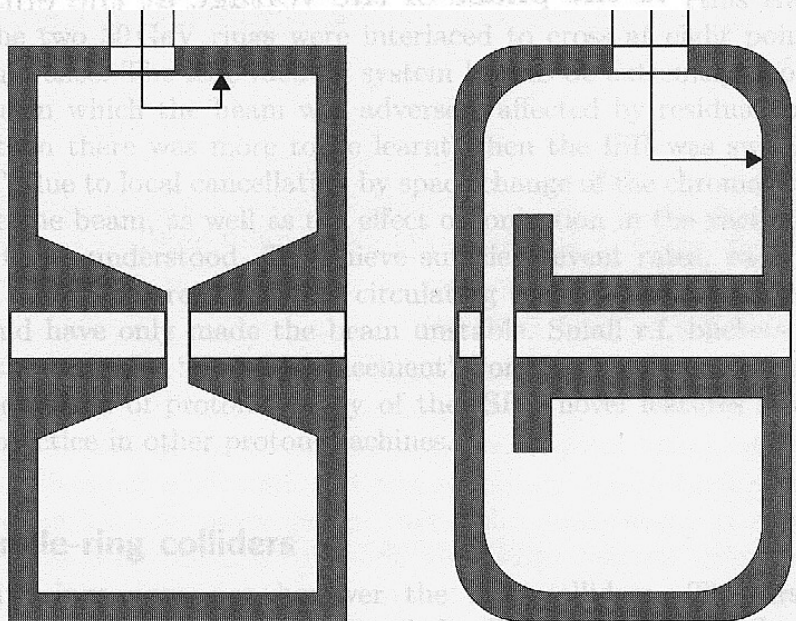
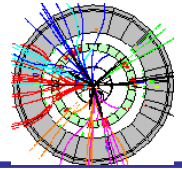


Fig. 10.15 Two examples of loop coupling.

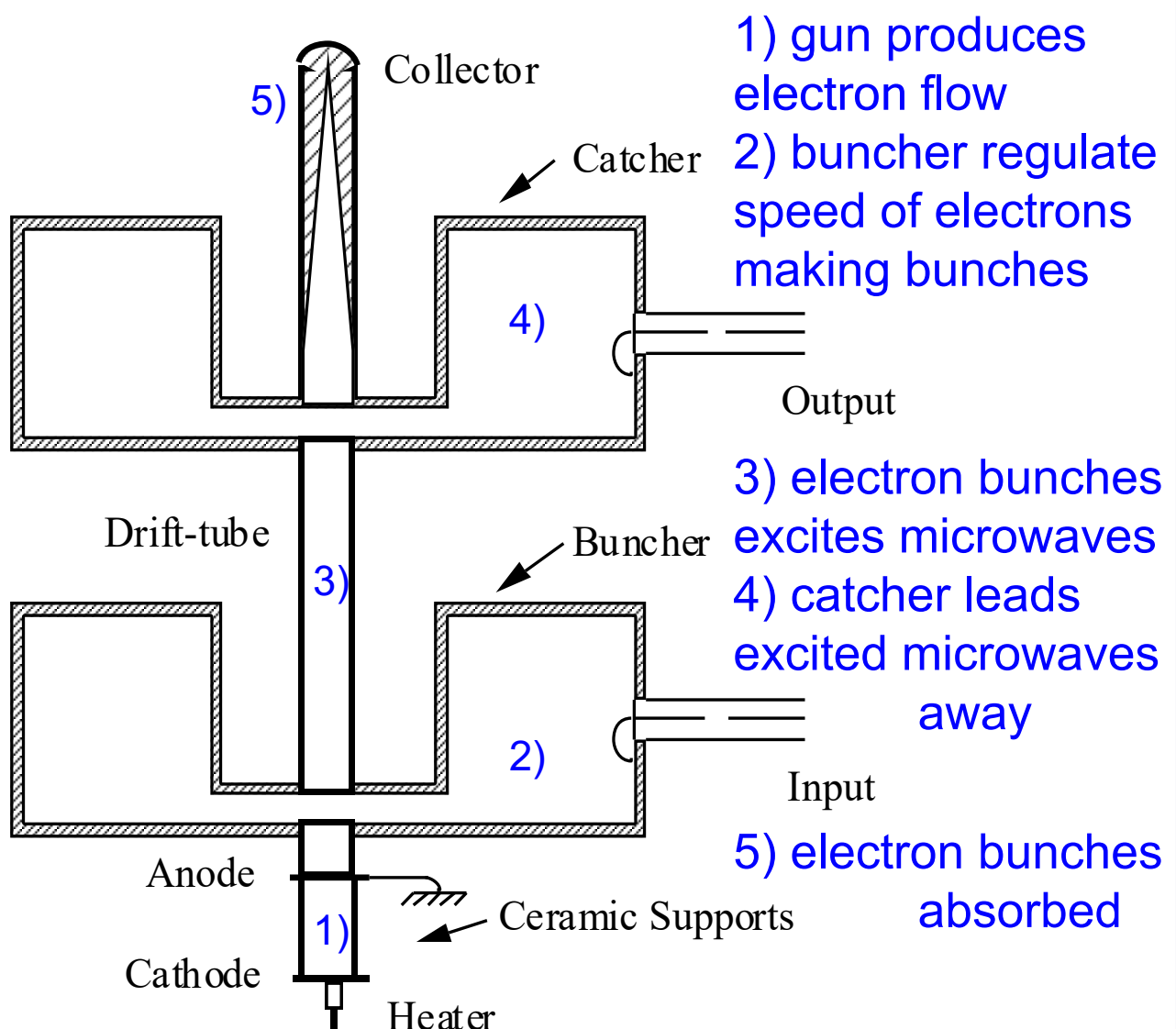


RF generation



Sinusoidal power to accelerating structures generated using resonant amplifiers. Mainly two types: triodes / tetrodes (wide frequency range but limited power) & klystrons (large power but limited frequency range)

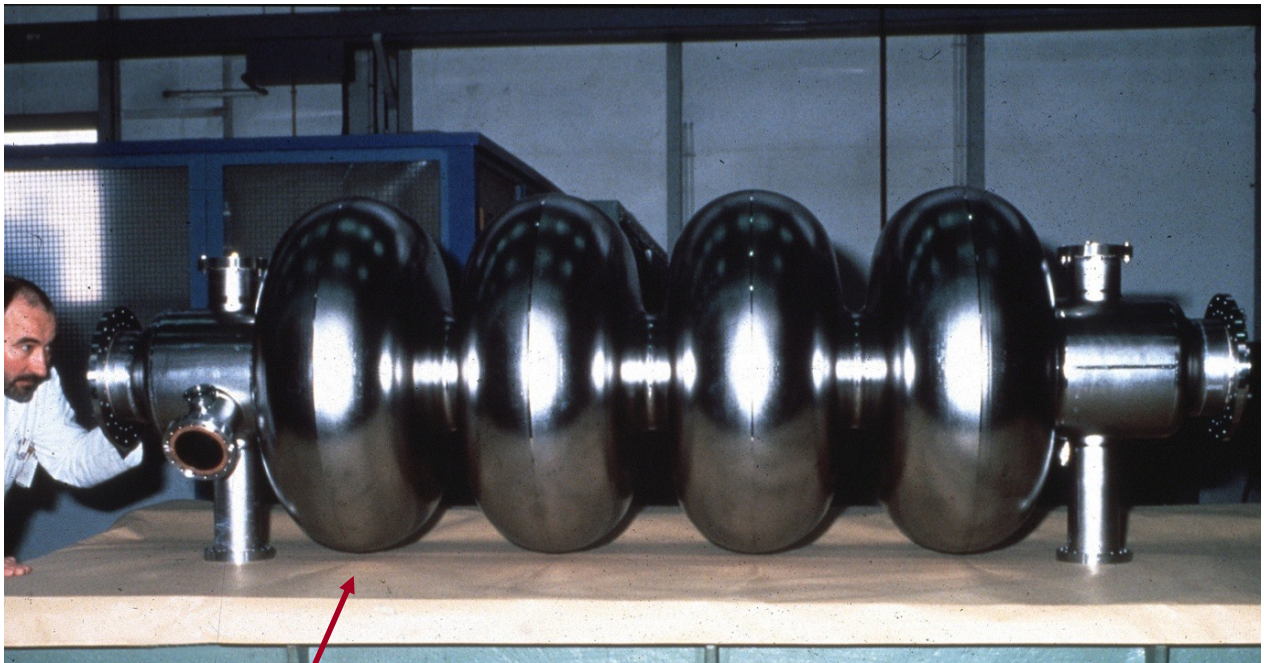
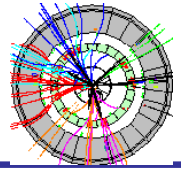
Klystron: intense electron gun - microwave generator (cf. microwave oven).



pulsed power as large as 50 MW
(\leftrightarrow triodes few 100 kW)

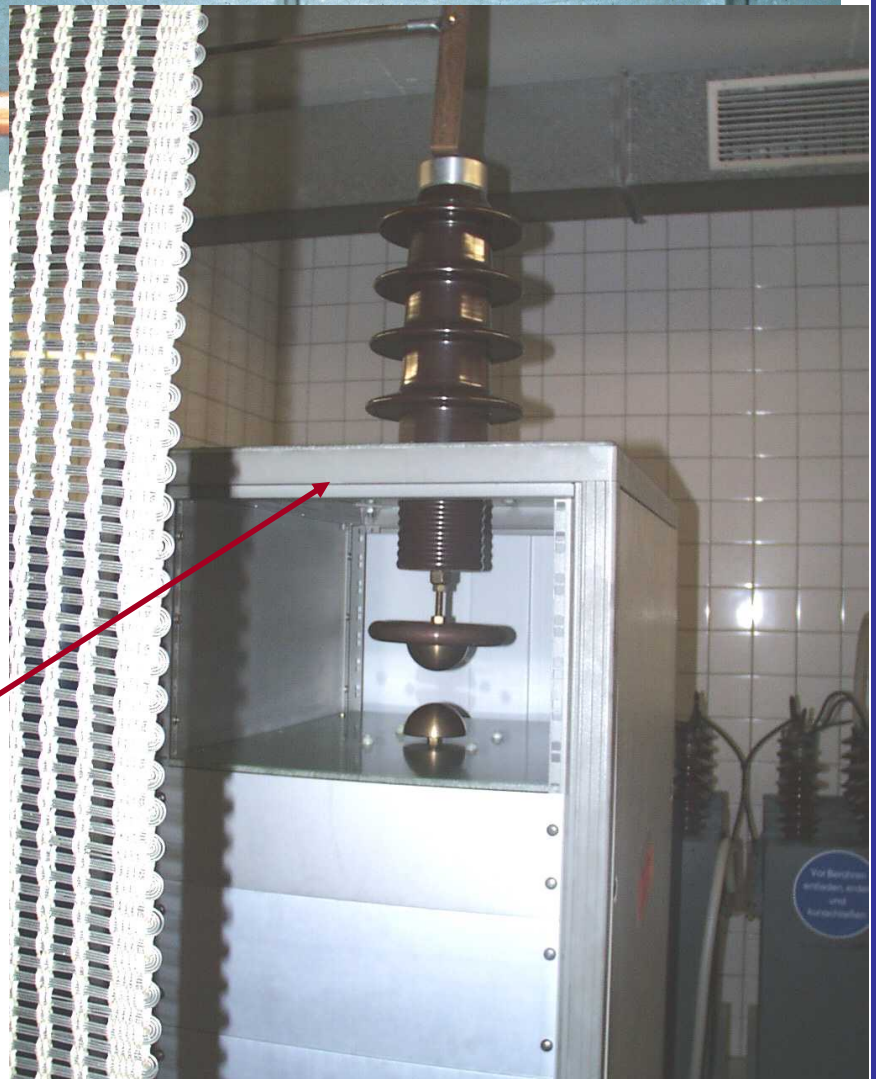


Picture gallery



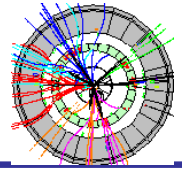
Superconducting
RF cavity used
for CERNs LEP
collider

A 208.2 MHz
klystron used
for the HERA
collider at
DESY





Closed-orbit distortions



Imperfections in guide field distorts the particles' orbit. Magnets cannot be made absolutely equal + other imperfections, such as position offsets, give rise to field errors. Let's examine effect of additional short dipole:

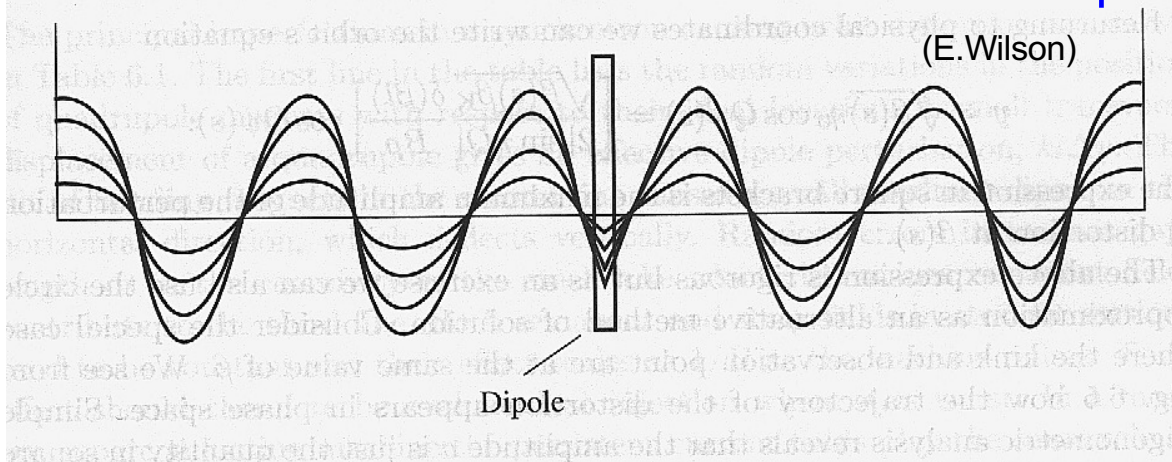


Fig. 6.3 Closed-orbit distortion as a dipole is slowly switched on.

- zero-betatron amplitude particle follows a distorted orbit. Distorted orbit **closed** & obeys Hill's equation, except at "dipole" follows normal betatron oscillations.
- finite-betatron amplitude particles oscillate around new orbit

to ease treatment of distortions we'll define new circular coordinates

$$x = x, \quad p = \beta x'$$

figure shows case of an accelerator with $Q = 27.6$. phase advance after one complete turn 2π multiplied by fractional part of Q .

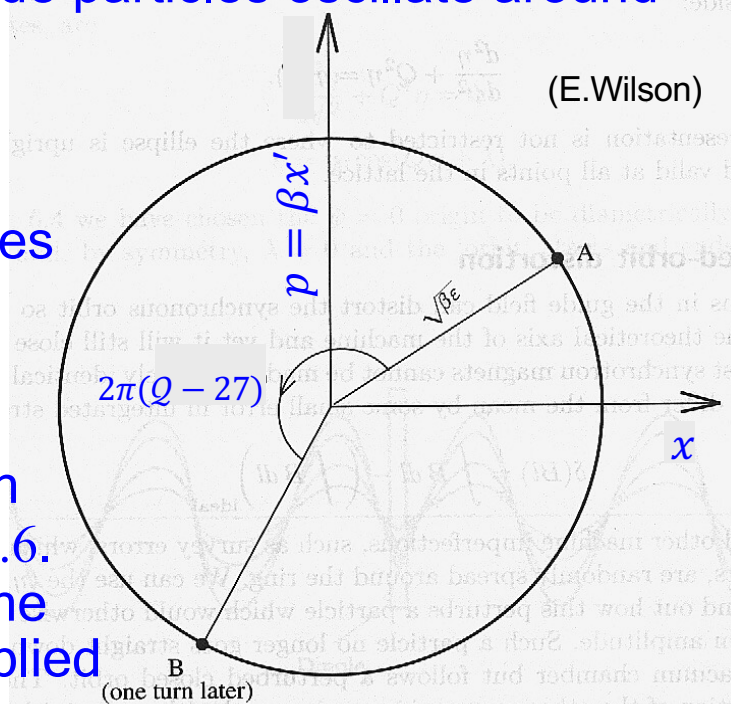
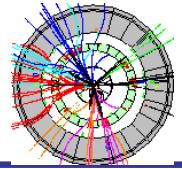
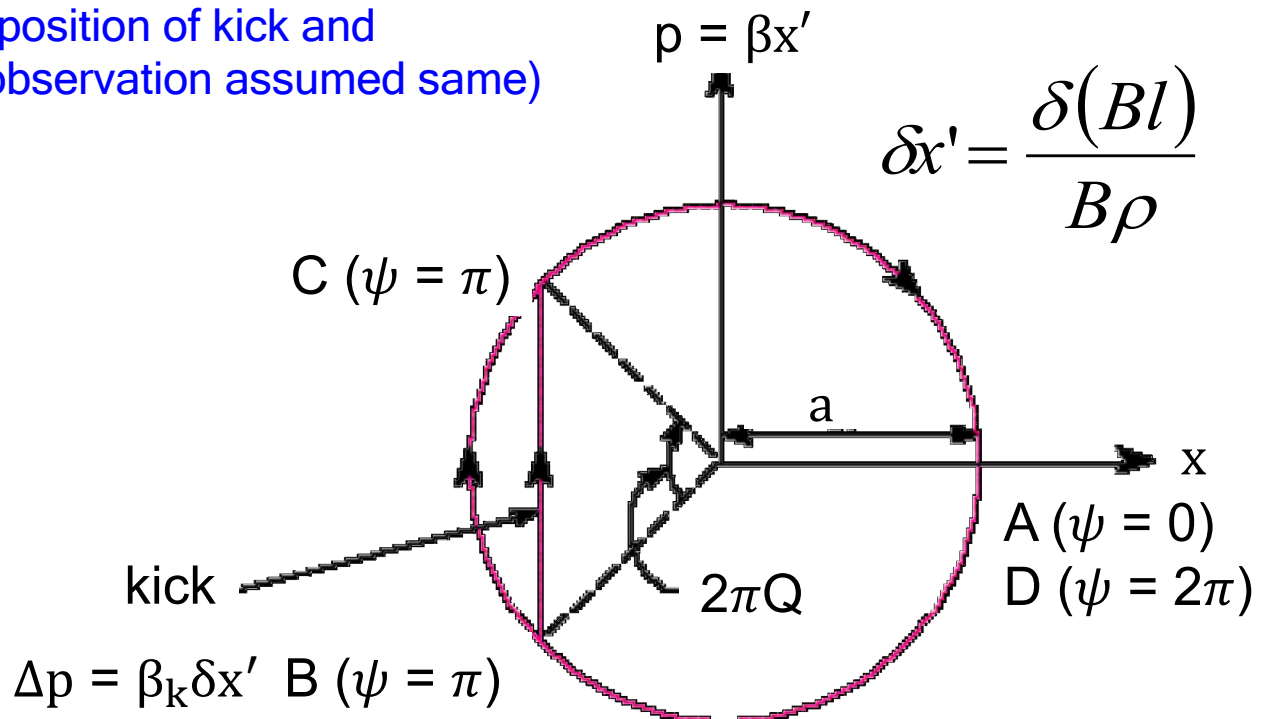


Fig. 6.2 Circle diagram (locus at F quadrupoles).



(position of kick and observation assumed same)



Tracing a closed orbit with a single kick for one turn using new circular coordinates. Path is ABCD.

$$\frac{\Delta p}{2} = \frac{\beta_k \delta x'}{2} = a \sin\left(\frac{2\pi Q}{2}\right) \Rightarrow a = \frac{\beta_k \delta x'}{2 \sin \pi Q}$$

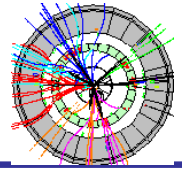
In other positions: $x_{\max} = a \sqrt{\frac{\beta(s)}{\beta_k}} = \frac{\sqrt{\beta_k \beta(s)}}{2 \sin \pi Q} \delta x'$

Solving Hill's equation for any position on ellipse gives:

$$x(s) = \left[\frac{\sqrt{\beta_k \beta(s)}}{2 \sin \pi Q} \right] \delta x' \cos \psi(s), \text{ where } \delta x' = \frac{\delta(Bl)}{B\rho}$$



Closed-orbit distortions



Multiple dipole distortions:

- reality: a random distribution of N dipole field errors. average over sine & cosine phases (gives factor $\sqrt{2}$). average value of offset of the closed orbit becomes:

$$\langle x(s) \rangle = \frac{\sqrt{\beta(s)}}{2\sqrt{2} \sin \pi Q} \sqrt{\sum_{i=1}^N \beta_i \delta x_i'^2}$$

- introducing an average field error $\langle \delta(Bl) \rangle$

$$\langle x(s) \rangle \approx \frac{\sqrt{\beta(s)\bar{\beta}}}{2\sqrt{2} \sin \pi Q} \sqrt{N} \frac{\langle \delta(Bl) \rangle}{B\rho}$$

Keeping distortions of closed orbit to minimum crucial otherwise available accelerator aperture significantly reduced. At F quadrupole amplitude function at largest \Rightarrow a kick close to F quadrupole has most effect on emittance. Used to put a safety factor 2 on accelerator aperture to accomodate distortions but modern accelerators cannot afford that & rely on closed-orbit steering with correcting magnets to make first turns.

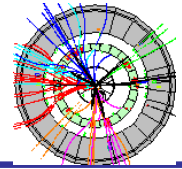
To illustrate potential problem with distortions, one can look at result of a Fourier analysis of a ΔB distortion:

$$\frac{x(s)}{\sqrt{\beta(s)}} = \sum_{k=1}^{\infty} \frac{Q^2 f_k}{Q^2 - k^2} e^{ik\psi} \quad \& \quad f_k = \frac{1}{2\pi Q} \oint \sqrt{\beta} \left(\frac{\Delta B}{B\rho} \right) e^{-ik\psi} ds$$

Magnification large when k near Q , infinite if $Q = k$ & beams lost. Each k value corresponds to a closed orbit.



Resonance condition



Orbit distortion amplitude:

$$x(s) = \frac{\sqrt{\beta(s)\beta_k}}{2 \sin \pi Q} \frac{\delta(Bl)}{B\rho} \cos \psi(s)$$

Infinite if $Q = \text{integer value or fractional}$ (beam receives kick at same phase on every turn & spirals outwards).

Working diagram of the SPS. Each line has a finite width proportional to strength of imperfection driving it. Strength usually proportional to n value of resonant condition.
NB! Beam a circle due to its spread in Q .

- simple resonant condition

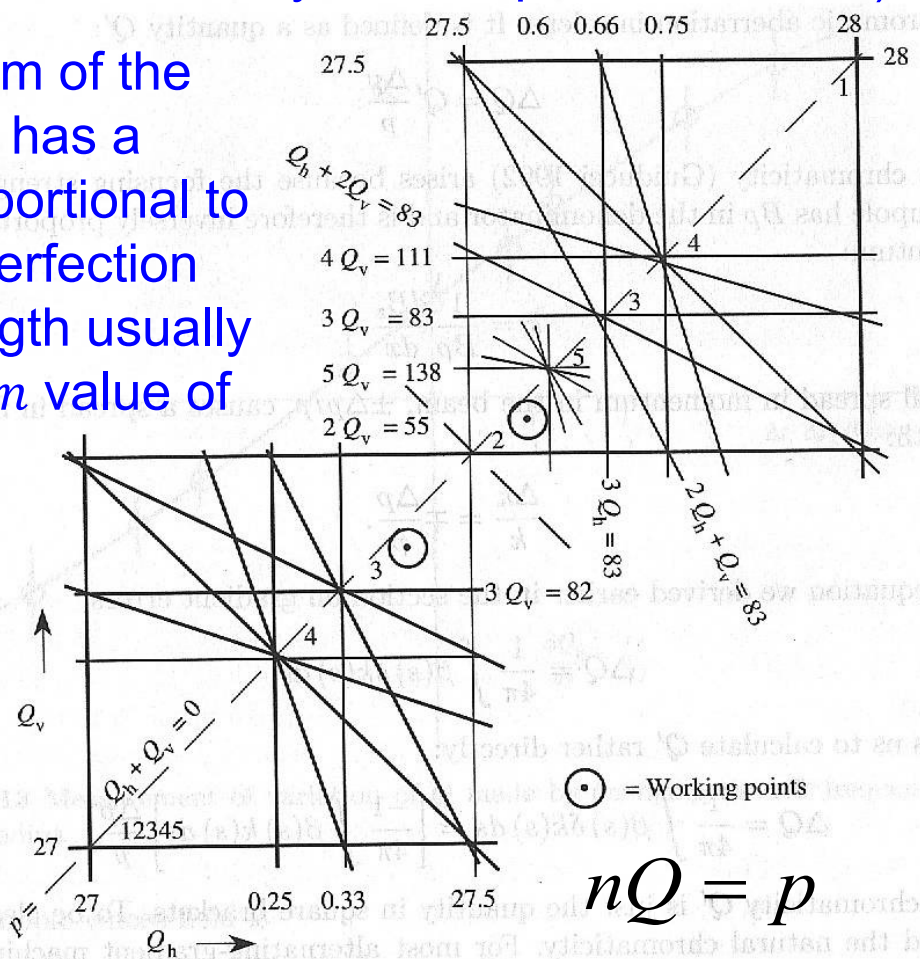


Fig. 6.12 SPS working diamond.

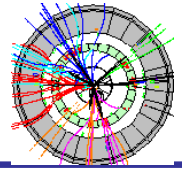
$$lQ_H + mQ_V = p$$

$$|l| + |m| = n$$

- defines a set of lines in the Q diagram for the n :th order resonance since both Q_H and Q_V have to be involved & this for each value of the integer p .



Sources of distortion



Sources of distortions :

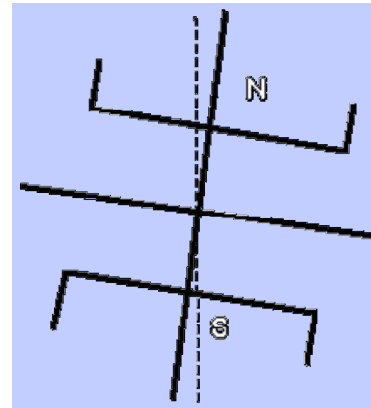
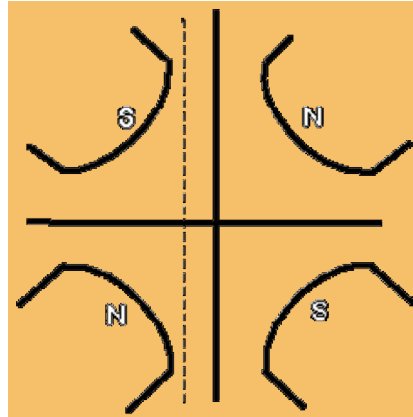


Table 1 $\Delta x / \Delta y$

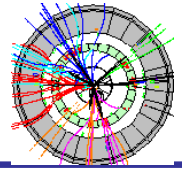
Δ

$\theta_i \approx l/\rho$

Sources of Closed Orbit Distortion

Type of element	Source of kick	r.m.s. value	$\langle \Delta B l / (B \rho) \rangle_{rms}$	plane
Quadrupole magnet	Displacement	$\langle \Delta x \rangle / \langle \Delta y \rangle$	$k_i l_i \langle \Delta x \rangle / k_i l_i \langle \Delta y \rangle$	x, y
Bending magnet (bending angle = θ_i)	Tilt	$\langle \Delta \rangle$	$\theta_i \langle \Delta \rangle$	y
Bending magnet	Field error	$\langle \Delta B / B \rangle$	$\theta_i \langle \Delta B / B \rangle$	x
Straight sections (length = d_i)	Stray field	$\langle \Delta B_s \rangle$	$d_i \langle \Delta B_s \rangle / (B \rho)_{inj}$	x, y

Persistent current fields in superconducting magnets in modern synchrotrons plays similar role as stray fields.
NB! $1/B$ dependence \Rightarrow effects largest at injection.



Effect of perturbed quadrupole on whole accelerator:

variables with subscript 0 = unperturbed values

unperturbed matrix:

perturbed matrix:

$$m = \begin{pmatrix} 1 & 0 \\ -[k_0(s) + \delta k(s)]ds & 1 \end{pmatrix}$$

$$m_0 = \begin{pmatrix} 1 & 0 \\ -k_0(s)ds & 1 \end{pmatrix}$$

ideal twiss matrix for one turn:

$$M_0(s) = \begin{pmatrix} \cos \mu_0 + \alpha_0 \sin \mu_0 & \beta_0 \sin \mu_0 \\ -\gamma_0 \sin \mu_0 & \cos \mu_0 - \alpha_0 \sin \mu_0 \end{pmatrix}$$

Fig. 6.11 Matrix representation of a small quadrupole, m_0 , subject to an error which is a component of the matrix for the whole ring, M .

perturbed twiss matrix for one turn:

$$M(s) = mm_0^{-1}M_0(s) = \begin{pmatrix} \cos \mu_0 + \alpha_0 \sin \mu_0 & \beta_0 \sin \mu_0 \\ -\delta k(s)ds(\cos \mu_0 + \alpha_0 \sin \mu_0) - \gamma_0 \sin \mu_0 & \cos \mu_0 - (\delta k(s)ds\beta_0 + \alpha_0)\sin \mu_0 \end{pmatrix}$$

$$mm_0^{-1} = \begin{pmatrix} 1 & 0 \\ -\delta k(s)ds & 1 \end{pmatrix}$$

change of $\cos \mu$:

$$\Delta(\cos \mu) = \frac{\Delta(\text{Tr } M)}{2} = -\Delta\mu \sin \mu_0 = -\frac{\sin \mu_0}{2} \beta_0(s) \delta k(s) ds$$

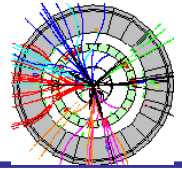
change of Q :

$$2\pi\Delta Q = \Delta\mu \Rightarrow \Delta Q = \frac{1}{4\pi} \int \beta(s) \delta k(s) ds$$

NB! change independent of phase at perturbation.



Transverse space charge



Particles inside a bunch see the electrostatic field of their neighbours. Below a simple analysis to estimate effect on transverse motion ignoring bunch structure of a beam.

Assume a cylindrical beam cross section. A proton at (r, ϕ) experience field & force (in proton coordinate system *):

$$E_r^* = \rho^* r^* / 2\epsilon_0 \quad F^* = eE^*$$

where ρ = charge density.

Transforming this to the laboratory system gives:

$$E_r = \rho r / 2\epsilon_0 \quad B_\phi = \rho r \beta / 2\epsilon_0 c$$

$$\Rightarrow \partial F_r = e(\vec{E} + \vec{v} \times \vec{B}) = \frac{e\rho}{2\epsilon_0}(1 - \beta^2)r = \frac{e\rho r}{2\epsilon_0\gamma^2}$$

δ of focusing force = δ of rate of transverse momentum:

$$\partial F_r = \frac{d}{dt}(E_T) = m\gamma \frac{d^2 r}{dt^2} = m\gamma(\beta c)^2 \frac{d^2 r}{ds^2} \Rightarrow \rho = eN / 2\pi RS$$

$$\frac{d^2 r}{ds^2} = \left(\frac{r_p N}{\beta^2 \gamma^3 RS} \right) r$$

S = beam cross section
 N = number of circulating protons
 $r_p = e^2 / 4\pi\epsilon_0 m_p c^2$

Hill's equation with a defocusing term k equal to bracket.

Using Q spread formula for gradient error obtain ($\bar{\beta} = R/Q$)

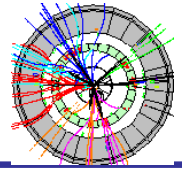
$$\delta Q \approx -\frac{\bar{\beta} k R}{4\pi} = \frac{-r_p R N}{2Q\beta^2 \gamma^3 S} > -0.25$$

N corresponding to $\delta Q = -0.25$ space charge limit
 Effect largest at injection.

Very approximative, for a more detailed analysis see e.g. A. Hofmann, proceedings of CERN accelerator school 1992, Jyväskylä, CERN 94-01.



Chromaticity



Steering of Q depends on careful regulation of quadrupole (& to less extent dipole) power. A large fraction of time in setting up large circular accelerators devoted to tuning Q to remain constant as field and energy rises.

quadrupole field strength: $k = \frac{1}{B\rho} \frac{dB_z}{dx} \propto \frac{1}{p}$

differentiating: $\Delta k/k = -\Delta p/p$

from gradient error analysis: $\Delta Q = \frac{1}{4\pi} \int \beta(s) \delta k(s) ds$

Enables estimate of Q spread from momentum spread:

$$\Delta Q = \frac{1}{4\pi} \int \beta(s) \delta k(s) ds = \left[-\frac{1}{4\pi} \int \beta(s) k(s) ds \right] \frac{\Delta p}{p}$$

Chromaticity Q' defined as factor relating Q with p spread:

$$\Delta Q = Q' \frac{\Delta p}{p} \quad (\text{similar to chromatic aberration in a lens})$$

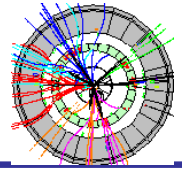
"Natural" chromaticity of most alternating-gradient machines:

$$Q' = -\frac{1}{4\pi} \int \beta(s) k(s) ds \approx -1.3Q$$

Total Q' can be larger than this due to other elements than quadrupoles (e.g. $Q' = -60$ at HERA proton ring with $Q \approx 31$). ΔQ can become as big as 0.10 in large electron synchrotrons (e.g. FCC-ee) with energy spreads of $\sim 10^{-3}$. This too large to avoid resonances & therefore must be corrected.



Chromaticity



Measurement/correction of chromaticity:

Chromaticity measured by offsetting RF frequency so that mean beam momentum changes & same time measure Q .

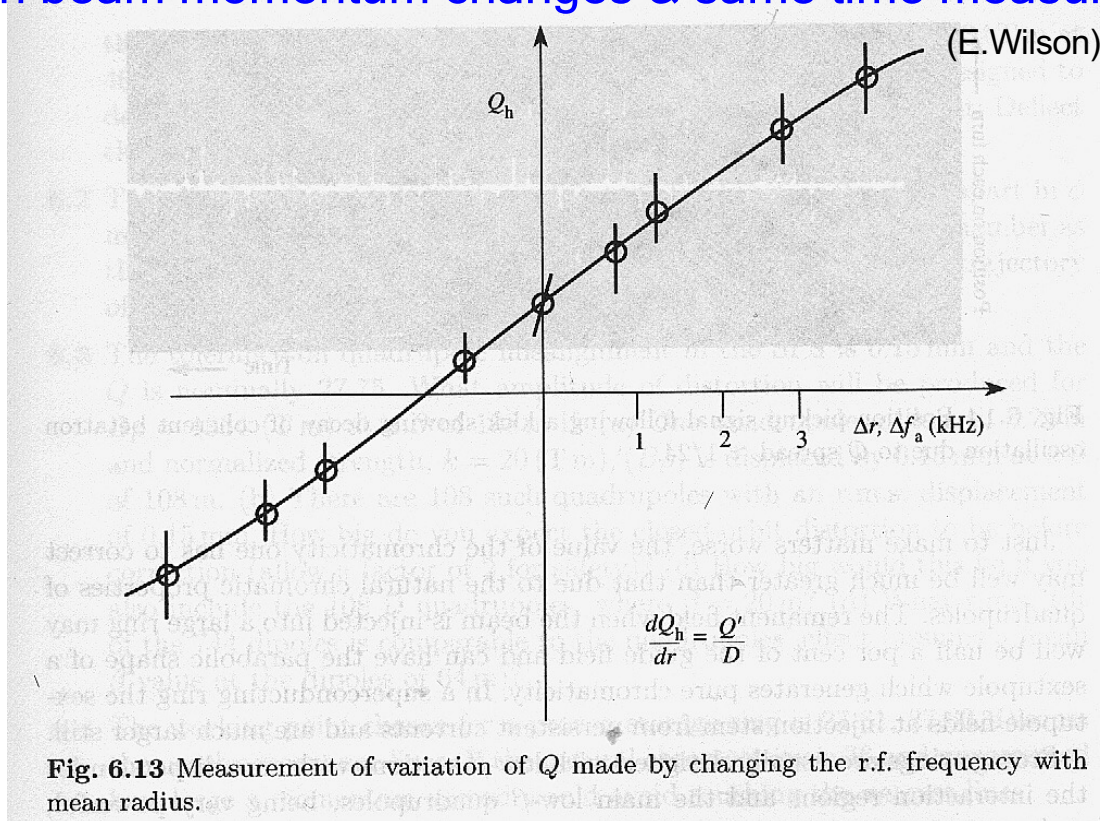


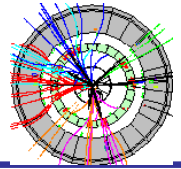
Fig. 6.13 Measurement of variation of Q made by changing the r.f. frequency with mean radius.

Too large chromaticities corrected by introducing focusing that gets stronger for higher ΔE -orbits \leftrightarrow a field with increasing gradient as function of radial position - adding a sextupole field $B_z = B''x^2/2$ using a sextupole magnet:

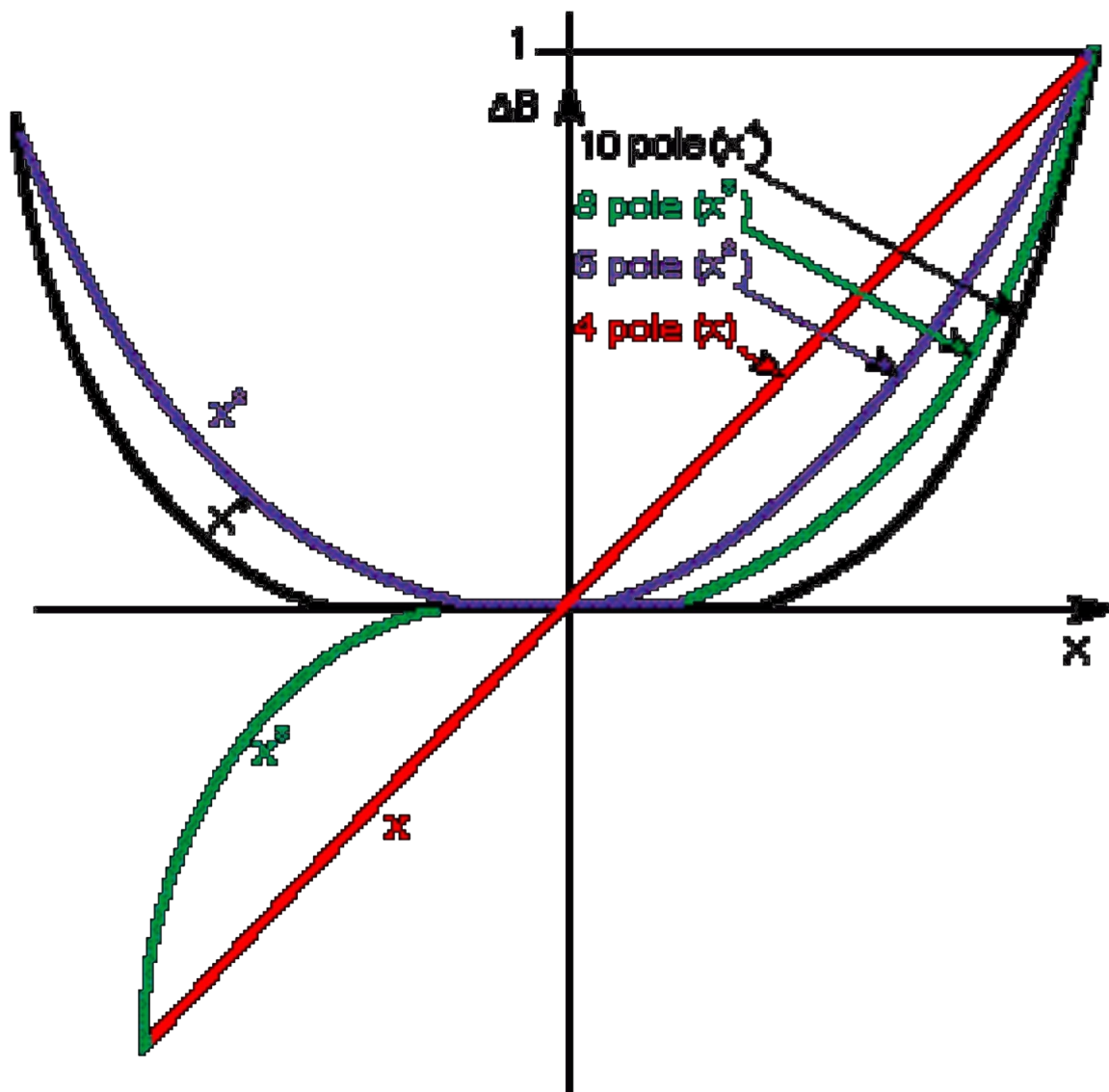
$$\Delta k = B'' D / B\rho \cdot \Delta p / p, \text{ since } x = D \cdot \Delta p / p$$

$$\text{Influence on } Q \text{ spread: } \Delta Q = \left[\frac{1}{4\pi} \int \frac{B''(s)\beta(s)D(s)ds}{B\rho} \right] \frac{\Delta p}{p}$$

To correct for chromaticity, the quantity inside the brackets must balance the natural chromaticity, both in horizontal & vertical planes with separate sextupoles close to the F and the D quadrupoles affecting mostly Q_H & Q_V , respectively.

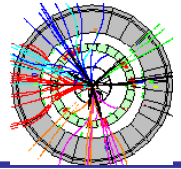


Multipole field shapes:

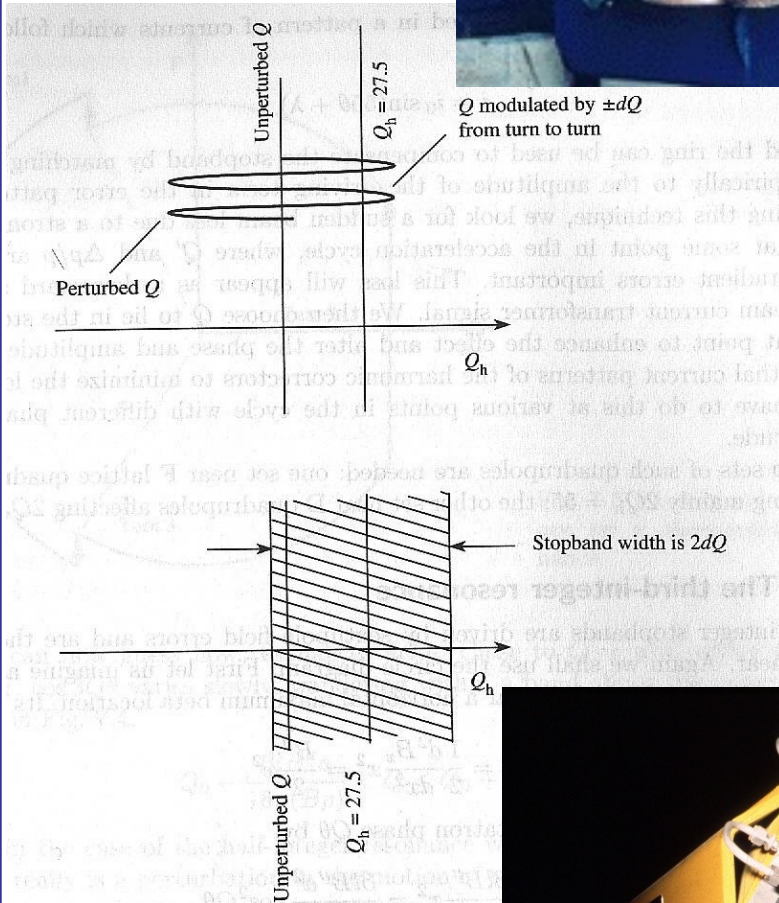
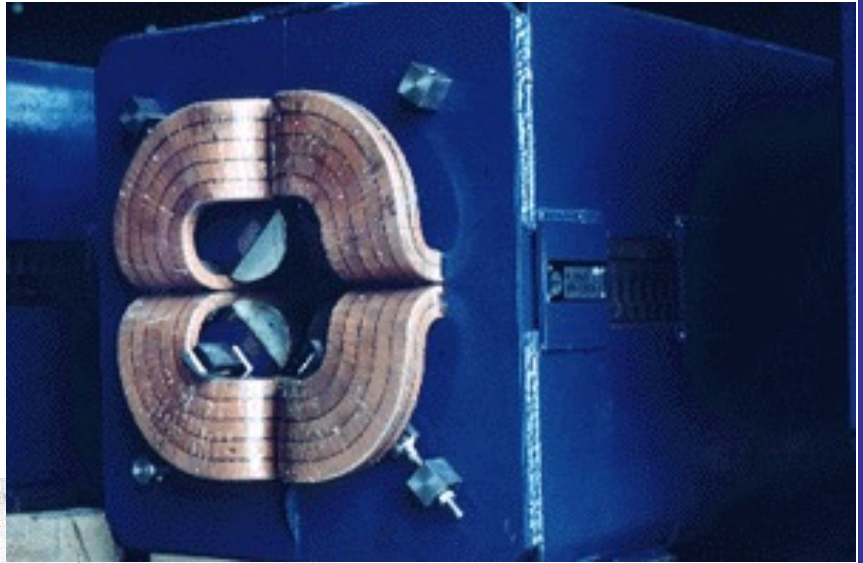




Magnets & stop band



A quadrupole magnet focusing the beam



quadrupole field errors lead to a modulated Q varying from turn to turn \Rightarrow define stop bands related to $Q \pm \Delta Q$

Fig. 7.4 Alternative diagrams showing pert

A sextupole magnet correcting the closed orbit

